TALLINN UNIVERSITY OF TECHNOLOGY
School of Information Technologies

Alfred Zelttser 142537

INVESTIGATION OF POSSIBLE CORRELATION BETWEEN THE CARDIAC PULSE WAVE PROPAGATION TIME AND BLOOD PRESSURE

Bachelor's thesis

Supervisor: Andrei Krivoshei

Ph.D.

Tallinn 2018

TALLINNA TEHNIKAÜLIKOOL

Infotehnoloogia teaduskond

Alfred Zelttser 142537

SÜDAME IMPULSSLAINE LEVIMISE AJA JA VERERÕHU KORRELATSOONI HINDAMISE VÕIMALUSTE UURIMINE QUADRA IMPEDANTS-SPEKTROSKOOPIA SEADME ABIL

Bakalaureusetöö

Juhendaja: Andrei Krivošei

Filosoofiadoktor

Tallinn 2018

Author's declaration of originality

I hereby certify that I am the sole author of this thesis. All the used materials, references to the literature and the work of others have been referred to. This thesis has not been presented for examination anywhere else.

Author: Alfred Zelttser

21.05.2018

Abstract

In this thesis was investigated the correlation between the time of pulse wave propagation and arterial blood pressure. To record the pulse wave, the bioimpedance measurement technology was used with applying the Quadra impedance spectroscopy analyzer. Quadra was used to measure the bioimpedance of arteries through two synchronous channels for the subsequent finding of a delay between pulse waves. The technology of Pulse Transit Time was investigated, which principle is determining the pulse wave propagation delay between two sites of arteria and the newer technology - Differential Pulse Arrival Time, when the delay between arteries of different length is determined. Of particular interest was the development of Bold Diagnostics in 2016, using photoplethysmography. According to their assertion, they managed to implement the Differential Pulse Arrival Time technology as a way of measuring pressure.

The purpose of this work was, in fact, verification of the attainability of such a result with the use of electrical biompedance sensors insteabd of photoplethysmography. To work with the measured Quadra signals, a MATLAB application was developed. Using the application, the measured data was filtered to separate a useful signal and to calculate the time delay between signals on two channels. A series of tests was carried out on several subjects to construct a correlation between the measured pressure at them and the calculated delay of the pulse wave. Were detected delays for both methods in the range from 0 to 40 milliseconds. Despite the extremely low sampling frequency (100 Hz) for such purpose, a some dependence was discovered. A certain correlation was found between the measured delay and the pressure of the subjects. Although the nature of the change requires more in-depth study, the viability of the method was identified.

This thesis is written in English and is 46 pages long, including 7 chapters, 22 figures and 10 tables.

Annotatsioon

Südame impulsslaine levimise aja ja vererõhu korrelatsooni hindamise võimaluste uurimine Quadra impedants-spektroskoopia seadme abil

Antud töös uuriti korrelatsiooni pulse laine levimise aja ja arteriaalse vererõhu vahel. Impulsslaine registreerimiseks kasutati Quadra impedantspektrograafianalüsaatorit kasutades bioimpedantsi mõõtmise tehnoloogiat. Quadra kasutati arterite bioimpedantsi mõõtmiseks kahe sünkroniseeritud kanali kaudu, et leida hilisem viivitus pulseerivate lainete vahel. Olid uuritud Pulse Transit Time tehnoloogia, mis defineerib pulsilaine levitamise viivitust kahe tuiksoone vahel ja uuema tehnoloogia - Differential Pulse Arrival Time, mis defineerib viivitamist erinevate pikkustega tuiksoone vahel. Eriti huvipakkuv oli Bold Diagnosticsi 2016. aasta kujundus, kus oli kasutatud fotopletüsmograafia. Selle tehnoloogia arendajate avalduste kohaselt, neil õnnestus rakendada tehnoloogiat Differential Pulse Arrival Time, kui rõhu mõõtmise vahendit. Käesoleva uuringu eesmärgiks oli tegelikult sarnase tulemuse kättesaadavuse kontrollimine, kasutades pletüsmograafia asemel elektrilisi biompedans andureid. Quadra poolt mõõdetud signaalidega töötlemiseks oli loodud MATLAB rakendus. Rakenduse abil mõõdetud andmed olid filtreeritud kasuliku signaali eraldamiseks ja oli väljaarvutatud ajaline viivitud nende vahel. Oli teostatud seeria katsetusi mitmetel subjektidel, et luua korrelatsioon mõõdetud surve vahel ja välja arvutada impulsi laine viivituse. Mõlema meetodi abil oli tuvastatud viivitused vahemikus 0 kuni 40 millisekundit. Vaatamata väga madalale proovivõtusagedusele (100 Hz) oli avastatud teatav sõltuvus. Oli leitud positiivne korrelatsioon mõõdetud viivituste ja subjektide surve vahel. Kuigi muudatuse olemus nõuab põhjalikumat uurimist, ilmnes meetodi elujõulisus.

Lõputöö on kirjutatud inglise keeles ning sisaldab teksti 46 leheküljel, 7 peatükki, 22 joonist, 10 tabelit.

List of abbreviations and terms

DPAT	Differential Pulse Arrival Time
DSP	Digital Signal Processor
EBI	Electrical Bioimpedance
ECG	Electrocardiography
FIR	Finite Impulse Response
ICG	Impedance Cardiography
PTT	Pulse Transit Time
PC	Personal Computer
PGA	Programmable Gain Amplifiers
POT`	Digital POTentiometer
PPG	Photoplethysmography
USB	Universal Serial Bus

Table of contents

List of figures

List of tables

1 Introduction

To date, electrocardiography (ECG) is the most common method of measuring the activity of the cardiovascular system (CVS). The principle of ECG is based on the detection of electromagnetic activity of the heart. The technique I use is based on impedance cardiography (ICG), which reflects the real work of the heart itself, and of the volume and blood pressure changes in the measurable artery segments. Blood spreads through the body of a person by pulsations, stimulated by contraction of the heart. By measuring the resistance of the blood in a specific area of the vessel in dynamics, we can observe the waveform of these impulses.

Impedance is a complex electrical resistance of a material, composed of usual resistance and reactance, which implies the inhibition of voltage (by capacitors) or current (by inductors). Bioimpedance, as the name suggests, is an impedance of organic tissues. Change of materials impedance can represent the change of its characteristics (like temperature, shape, size, chemical composition, etc.) In this thesis considered change of bioimpedance as a derivative of influenced parameters as cross-sectional area, indicating a change in the blood pressure on the walls of the artery. The measured resistance of the artery, in dynamics, will gives a rheogram for a particular section of the circulatory system. Since the work implies the impedance measurement from both wrists or from two parts of the forearm – part of research is analyzing of time delay between signals from each hand.

2 Measuring idea and principles

2.1 Impedance measurement

Impedance is a physical quantity that characterizes the ability of a conductor to impede the flow of electrical current. Unlike resistance, impedance also includes reactance in a complex form. Resistance is determined by the material, length and width of the conductor. The reaction consists of two parts, inductive X_L and capacitive X_C. X_C inversely depends on the conductor capacitance and frequency, and X_L directly depends on the inductance and frequency. Since the capacitive part is subtracted from the inductive one, any impedance is capacitive or inductive. Capacitive reactance is higher the higher the frequency of the signal, and the inductive the lower the higher the frequency. In addition, reactivity creates a phase shift of ± 90 degrees between voltage and current in the conductor section. Negative phase is created by the capacitive reactance when the current is ahead of the voltage. Inductive reactance creates a positive phase shift when the current is behind the voltage. Impedance is defined as the root of the sum of squares of resistance and reactivity [7].
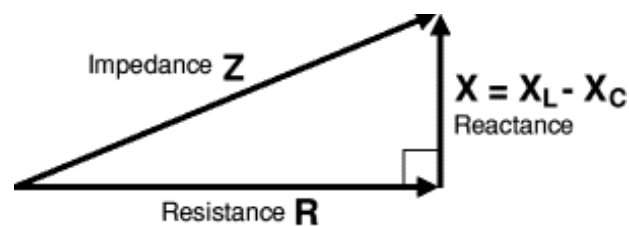
Figure 1. Graphical representation of impedance [7]

$$Z = \sqrt{R^2 + X^2} \quad \textbf{Impedance equation } (\Omega)$$

$$X = X_L - X_C \quad \textbf{Reactance equation } (\Omega)$$

$$X_C = \frac{1}{2\pi f C} \quad \textbf{Capacitive Reactance } (\Omega)$$

$$X_L = 2\pi f L \quad \textbf{Inductive Reactance } (\Omega)$$

$$Z = \sqrt{R^2 + (2\pi f L - \frac{1}{2\pi f C})^2}$$ **Detailed impedance equation**

Z – Impedance (Ω)	**X – Reactance (Ω)**
R – Resistance (Ω)	**C – Capacitance (F)**
f – Frequency (Hz)	**L – Inductance (H)**

There are two most common methods of measuring impedance. The first is realized according to the impedance formula - to calculate the impedance, you need to know capacitance and inductance in addition to the resistance measured by the Ohmmeter. By measuring these two parameters, you can calculate the impedance by hardware. Such devices are circuitry more complicated due to the combination of three measuring instruments. Their main problem lies in a narrow range of measured values [8].

The second method measures the impedance at a particular frequency. It is the method used by the device that performs measurements in this investigation. By creating alternating current on the load by the oscillator, another pair of leads measures voltage and current. Voltage is divided by the current and the value of the real impedance is obtained. The main limitation of this method is that it can measure impedance only at fixed frequencies, in contrast to the first method, which allows calculating the impedance for any frequency. However, for the purposes of this research, only one frequency is sufficient [8].

2.2 Bioelectrical impedance

The human body, like any material, basically, is a conductor. Because the human body consists of completely different tissues - the resistance of its various parts is also different. Moreover, the structure of the tissues differs in addition to the resistance they also have a reactance. Reactance in the human body has a capacitive type. This situation is due to the fact that multiple low-resistance isolated parallel conductors in the body are practically absent. In other words, in the human body are no equivalents to inductors or their inductance is insignificant.

The situation with a capacitive reactance is different. In the human body there are compounds representing two closely spaced isolated sections of the conductor, which are, in fact, equivalent capacitors. The most common of these is the cell membrane, which isolates the intercellular space from the cell itself. Organic tissue remains conductive at low frequencies by moving the current around the cells through the intercellular fluid. In this case, the resistance is increased by narrowing the overall width of the conductor and increasing the current path [12].
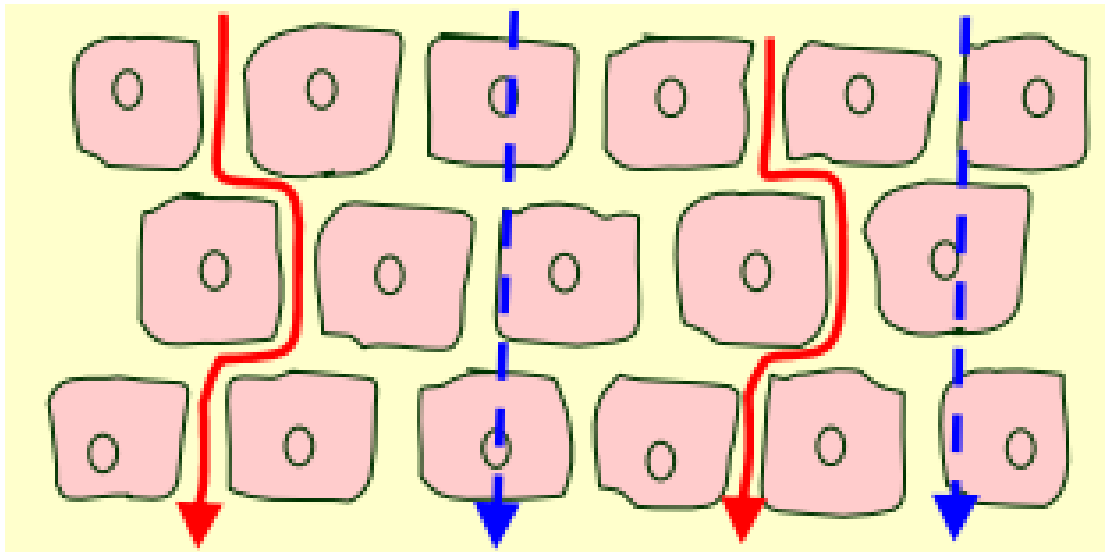
Figure 2. The paths of current flow in the cellular space at low (red) and at high (blue) frequencies [12]

In addition, a separate section of nerve cells (neurons) possesses a capacitive reactance. Neurons consist of two parts of the axon and dendrite, between which is a narrow (50 nm) synoptic gap. At a time when the neuron is at rest (between the axon and the dendrite neurotransmitter do not propagate), it is a small capacitor. Neurons during excitation also change the resistance, filling the synoptic space with neurotransmitters, which can also affect the measurement results [13].
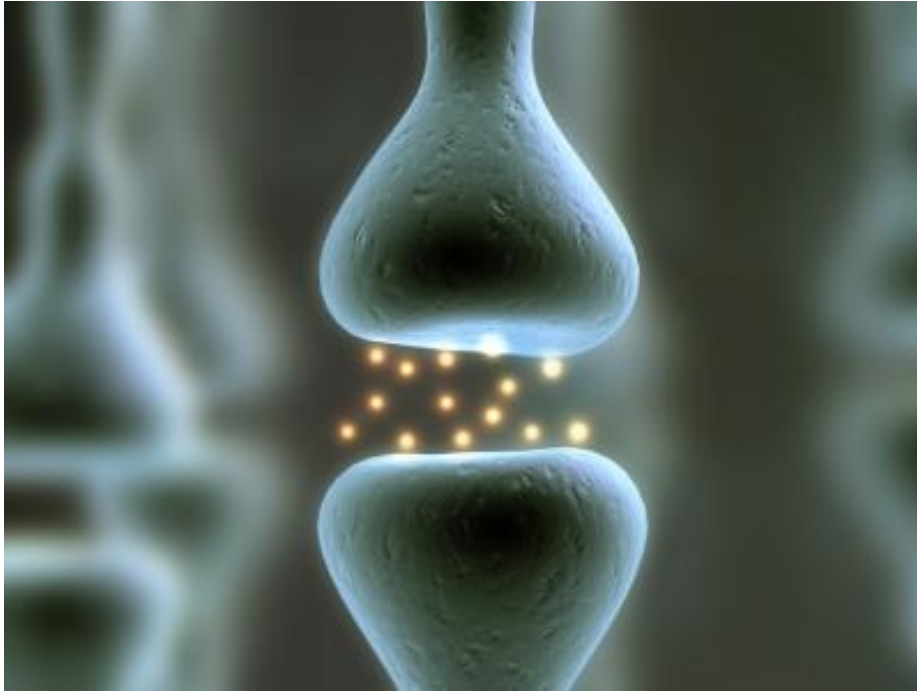
Figure 3. The image of synapse and neurotransmitter and distributed in it [13]

The effect of capacitive reactance, although present, is generally insignificant. Further, its influence can be seen on the phase-vs-frequency response curve. It can be seen that the phase shift along the entire width of the spectrum has a negative sign, which indicates the prevalence of the capacitive component (since the current signal is ahead of the voltage signal).

In our measurements, resistance is more important. It is, primarily, his change indicates the density of the blood flow. Resistance of blood is quite low in comparison with most other tissues, therefore the amplitude of the measured oscillations will be very small relatively to the base. Muscles, like blood, have low resistance, but their reduction significantly affects the value of impedance, therefore, during measurement, muscles must be relaxed. The skin resistance though is relatively large, but it is not affected by significant changes [12].

In this work, the impedance is measured on the skin areas to which the arteries are most closely located. Thus, the greatest change in impedance at a given site is due to a change in arterial pressure in this area. The fixed pulse wave has a definite shape. The first half of the pulse has a sharp rise and then a small, but a sharp decline. This interval is the response of the systolic period of the heart. At this point, both ventricles

contract and the discharge of blood into the aorta. The pressure level at the peak of this period is called the systolic or upper pressure. The second half of the pulse after a slight rise (dicrotic peak) starts to smoothly descend to the minimum pressure level. This part of the pulse corresponds to the diastolic period of the heart. During this period, all the cardiac chambers are relaxed and the heart is filling with blood. The pressure at the lower point of the period, right before the start of a new systolic front, is called diastolic or lower pressure [14].
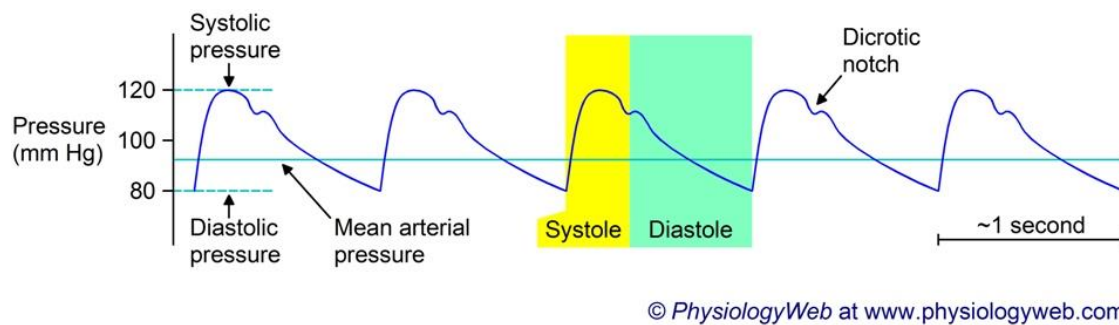
Figure 4. The pressure curve with the systolic and diastolic parts of a pulse wave [14]

2.3 Pulse Transit Time

Pulse Transit Time (PTT) is a technology for measuring human pressure, based on the time of pulse wave propagation along the artery. The principle of the method is that the pressure depends on the velocity of the pulse wave propagation through the vessels, and the velocity, in turn, determines the time of path of the artery by the pulse wave. To obtain a pulse wave signal, photoplethysmography (PPG) technology are widely used. It detect the change in the pulse wave with the help of an optocoupler placed around a blood vessel, and determine the density of the blood flow in time. There are other types of sensors, one of them is impedance sensors, which is used in this work. By placing the electrodes in different areas of the skin along the artery, the impedance change caused by the change in the flow density is measured and the time difference between similar values is analysed [3].
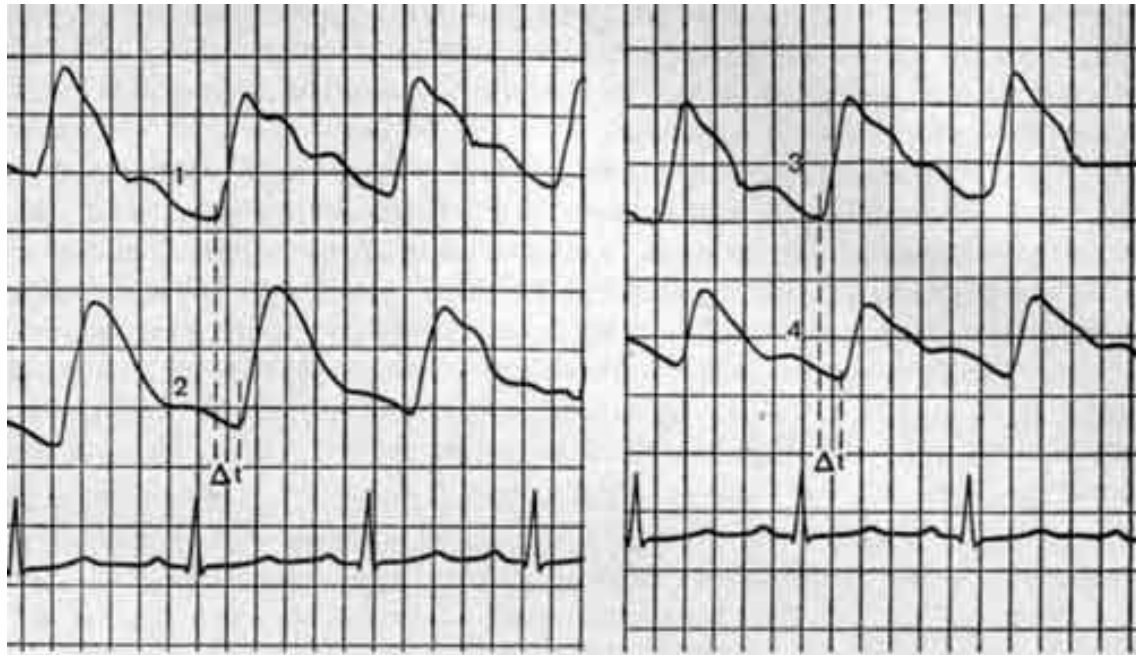
Figure 5. A sphygmogram illustrating the delay between pulse waves [10]

There are different ways of placing sensors to analyze the delay time. In my research, I chose a site at the base of the wrist where the radial artery passes, and the segment of the arms bend where the brachial artery passes into the radial and ulnar artery. The distance between these two segments is approximately 20 centimeters in an adult. Considering that the speed of propagation of a wave in an adult is close to 10 m/s, then the time of path of this segment fluctuates about 20 ms [9].

2.4 Differential Pulse Arrival Time

Differential Pulse Arrival Time (DPAT) - is nothing more than the development of the idea of PTT. In this method, not the pulse wave Path time on a length of artery is measured, but the difference in the transit time of different length arteries. It is assumed that with a change in pressure and, correspondingly, the propagation velocity of the pulse wave, the time delay between two waves passing through the different arteries changes too [1].

The specific DPAT method was created and patented by Bold Diagnostics in 2016, with which they won the contest "Create the Future 2016" [2]. The company's implementation is based on the estimation of the delay between the left and right radial

arteries. This delay is caused by the distance between the brachiocephalic artery, which goes to the right arm (through the branching right subclavian artery), and the left subclavian artery that goes to the left arm [1]. Because the brachiocephalic artery is located in the aorta closer to the heart than the left subclavian artery - the path and propagation time of the pulse wave along the arteries of the right arm is presumably smaller than for the left one. The length of the aortic arch (the distance between the brachiocephalic artery and the left subclavian artery) is about 5 cm, and the speed of the pulse wave in the aorta varies around 5 m/s. Thus, the delay between hands varies around 10 ms [11].

.
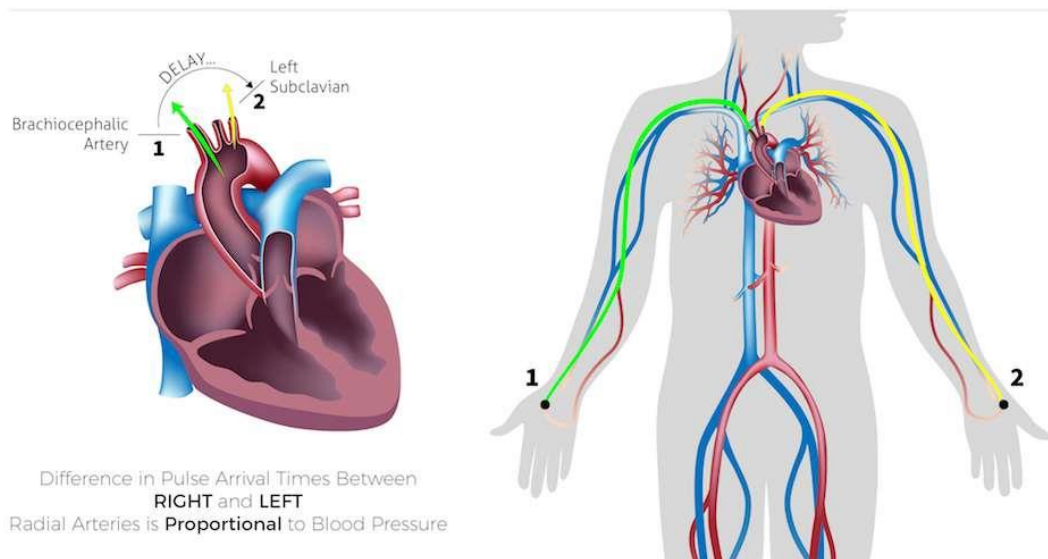
Figure 6. Illustration of delay cause [6]

The DPAT method, created by the Bold Diagnostics as sensors for recording the pulse waves, used PPG. In my research, the goal is to achieve a similar result by Electrical Bioimpedance (EBI) using the Quadra spectroscopy impedance analyzer. The Quadra sampling period is 10 ms, which does not allow a precise determination of the delay, but will allow us to determine the trend of the delay.

3 Equipment review

3.1 Impedance Spectroscopy Analyzer – Eliko Quadra

Eliko Quadra is a compact device designed to measure impedance by Eliko in collaboration with Tallinn University of Technology. Quadra uses a USB interface for data transferring with a data rate of up to 12 Mbps. Power is provided by the same USB interface or a battery for 8 hours. Since the device is still not designed for autonomous operation without connecting to a PC, the battery acts as a source of noise-proof power. Quadra contains a Digital Signal Processor (DSP), which provides generation of waveforms of 15 frequencies: 1 kHz, 2 kHz, 3 kHz, 7 kHz, 11 kHz, 17 kHz, 23 kHz, 31 kHz, 43 kHz, 61 kHz, 89 kHz, 127 kHz, 179 kHz, 251 kHz, and 349 kHz. The exciting signal is transmitted from the DSP to the two outputs going to the load, via the digital potentiometer (POT). The potentiometer has 200 positions in the range from 0.4 V to 7.5 V [4].
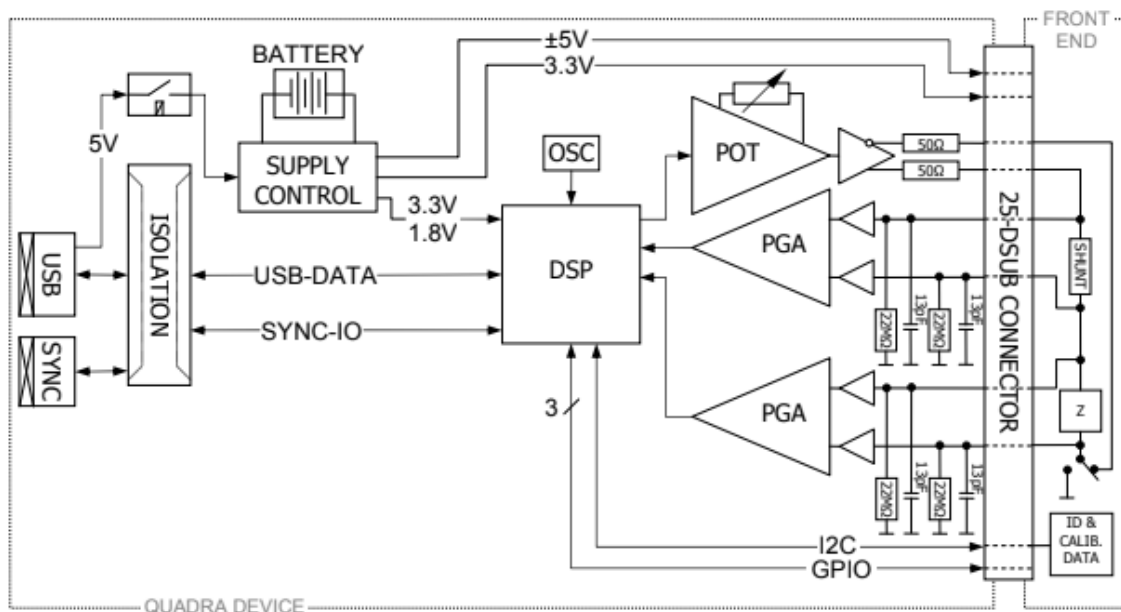
Figure 7. Quadra block diagram [4]

Between the terminals of the excitation signal, a shunt is sequentially located, from which the current in the circuit is measured, and the load measured by the device on which the voltage is measured. Each of the measured parameters is amplified by Programmable Gain Amplifiers (PGA). Each of the PGA has four gain levels: x1 (repeat

signal), x2, x5, and x10. The current is measured using a current-to-voltage conversion circuit, for further operation of the DSP with a value. When the samples of voltage and current come into the DSP, the impedance of the load is calculated according to Ohm's law and the phase shift between them is analyzed as well [4].

The device is equipped with a front-end adapter for converting the signal and connecting the electrodes. In our case, an adapter is used that plays the role of a hub creating four parallel channels, which are connected by a digital switch.

3.2 Quadra Front-end adapter

In addition to the head unit itself, Eliko Quadra requires an expansion adapter, various modifications of which are also provided by Eliko.
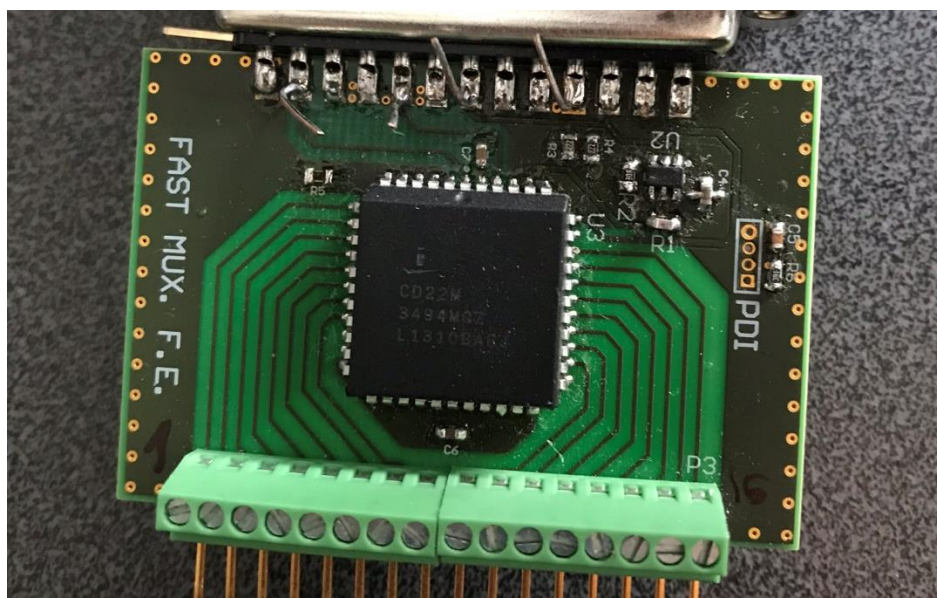
Figure 8. Photo of the front-end adapter from the side where the switch is located

For Quadra, there are a number of front-end adapters for different purposes. In our case, since we needed to measure the signals from two hands, we used an adapter based on the cross-point switch CD22M3494MQZ. The switch has 8 to 16 pins for connection and 128 switching inputs (decoded from combinations of seven inputs) [5]. On the side of the eight inputs, a pair of excitation terminals are connected, a pair measuring current and a pair measuring voltage. On the side of the 16 outputs, the arrangement of 4 channels of 4 outputs (the exciting current pair and the voltage measurement pair). The sequence and duration of the external channels connection is

set by the controller located on the adapter card and programmable via the user interface on the PC. Access to the master controller is via the DSP using the General-Purpose Input / Output (GPIO) interface.

Each of the four channels is switched in time. The manufacturer recommends a minimum measurement duration, taking into account transients, 4 ms. In practice, a time of 5 ms was chosen, since this time provides sufficient stability of the measurement, in contrast to 4 ms. Taking into account that only 2 channels were used from 4 channels, the sampling frequency was equal to 100 Hz (twice less than for one channel).
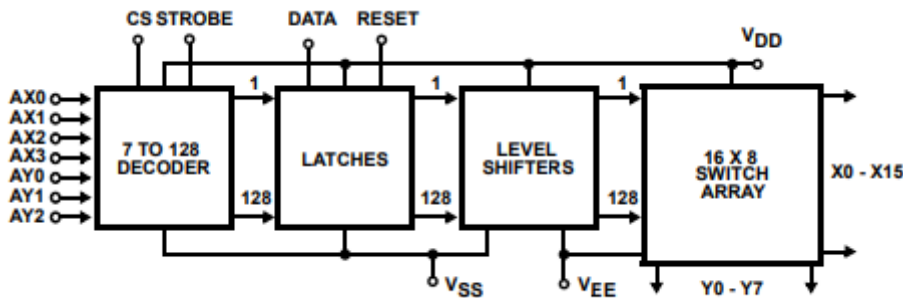
Figure 9. Block diagram of the switch CD22M3494MQZ [5]

3.3 Assembly adaptations

To connect the leads of the front-end adapter to the subject are uses connecting wires and ECG electrodes. Eight wires are connected to the first two channels of the adapter using pins at the ends. Four wires per channel, the first two channels, in turn, are on the left side of the adapter when viewed from the side of the switch. On the other side of the wires are snaps for fastening to the electrodes. It is important to ensure that the wires are placed on the hands of the subject in the appropriate connection order. The first and fourth leads on the channel are responsible for the excitation signal, the second and third for the voltage measurement (the same placement as for the measured load). To avoid confusion it is advisable to use wires of different colors.

21
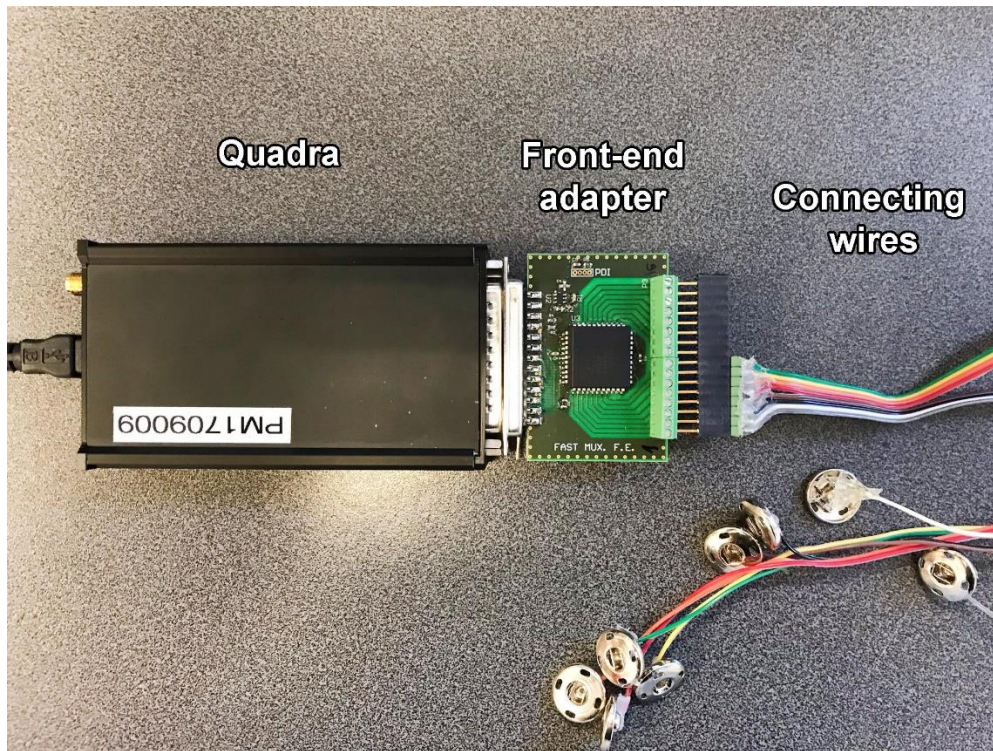
Figure 10. View of the assembled device with the names of its parts

The intermediate link between the wires and the subject is adhesive electrodes. Each electrode has a metal stud tightly connected to it, for which snap of wire is grasped. To fix the electrodes on the subject, the conductive part is embedded in a sticker, which should cut off on one axis to reduce the distance between the electrodes. The part, which connects the skin of the subject with the stud, consists of a highly conductive gel with. During the test, various types of electrodes were used, which did not significantly affect the signal quality. It is important not to allow the gel to dry out, so that its conductive properties are not lost.

Figure 11. Adhesive electrodes

4 Measurement procedure description

To obtain a qualitative and constant signal, the measurement procedure must be standardized and properly prepared. The first thing to do is to have all the "tools" for implementing measurements:

Software required:

- Software for Eliko Quadra, including the drivers required for the device.

- The program on LabVIEW, provided by the Institute of Electronics which allows to track and adjust the signal in real time on four channels (instead of the one available in the device by default), created by the front-end adapter based on the switch CD22M3494MQZ.

Hardware required:

- 1PC with operating system Windows XP or newer, USB 2.0 / 3.0 port.

- The device for measuring impedance - Eliko Quadra.

- Front-end adapter based on the switch CD22M3494MQZ.

- Beurer BM 58 pressure measuring device.

Assembly adaptations:

- Adhesive electrodes of the right size (indicated below).

- Eight wires, for connecting the output of the switch and the electrodes by snaps.

4.1 Software preparation

The measurement program provided with the front-end adapter is written in the LabVIEW environment and allows you to monitor, configure and store the measured signals. Launching the program to start the measurements is possible in the control panel in the upper right corner of the window. In the same toolbox, there is a button for restarting the program, emergency stop and pause. In area **A**, there is a curve of the frequency response of the signals. There is also a sampling time field (Scroll.ms), standard stop button, the number of channels (MUX position) and which ones should be displayed on the chart. Channels should be set to two, and the length of the sample - 5 ms. To the right of the graph is the choice of the frequency of the displayed signal. The recommended frequency for me to set is the 23 kHz (this frequency was chosen for further processing), because it was the most accurate signal during operations.
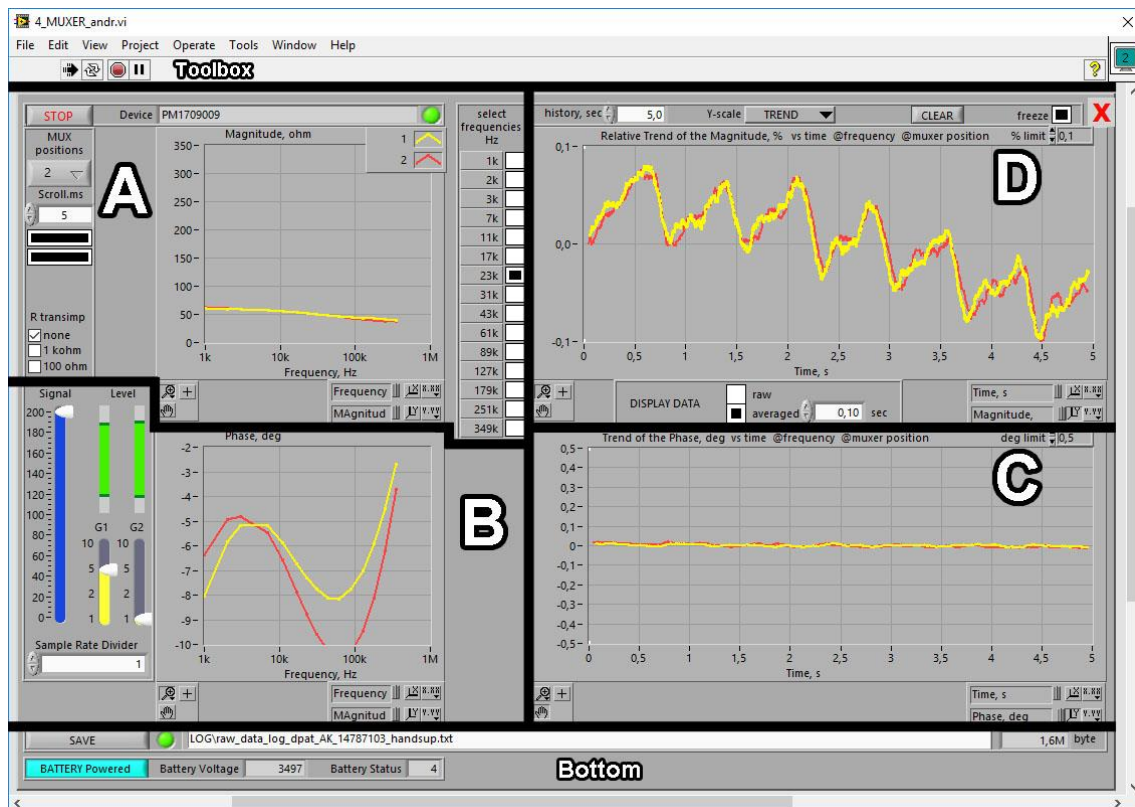
Figure 12. Screenshot of the LabVIEW program's window for monitoring the signals.
A – Frequency response, B – Phase-frequency response, C – Phase-frequency response, D – Time domain signal

In area **B** there is a phase-vs-frequency response plot. To the left of it is the PGA and POT gain control unit. The blue scale determines the level of the excitation signal. The two yellow bars G1 and G2 show the gain level for the measured current and voltage. G2 should always repeat the signal (stand on the unit), G1 should be set to 2 or 5. The level of the excitation signal is best to set as much as possible, as long as the amplification of the input signals does not exceed the allowable limit. The degree of amplification can be tracked along the green bands with the inscription "Level" above the voltage regulators. The longer the band, the higher the gain of the measured signal. If red lines appear at the ends of the bands, the measurement limit is exceeded.

In area **C**, a phase-vs-time plot is located. This curve characterizes the level of reactance, but also to some extent, resistance oscillations. This curve tells about the predominance of the capacitive component, its share at different frequencies. The curve shows that at a frequency of slightly less than 100 kHz the phase reaches -10 degrees. According to the formula (1),

$$\frac{X}{Z} = |\tan(\varphi)| = |\tan(-10)| \simeq 0.18 \tag{1}$$

which in turn means that the reactance is 18% of the resistance. This gives some idea of the maximum impact of reactance on the impedance.

In area **D** is located an amplitude-vs-time plot. It is the one plot used for observation of oscillations' shape. Under the graph are buttons for displaying raw and / or averaged (filtered) signal. Nearby is the field for selecting the time by which the signal is averaged. It is better to focus only on the average signal for a simpler perception, and for the averaging time the default interval of 0.1 ms is quite suitable. Above the graph is a field for selecting the displayed time interval, scale type along the y-axis (trend or absolute), the ability to clear the measurement buffer and freeze the measurement frame.

In the left part of the window's bottom is a button to start (and finish if started) the signal recording. Below it, there is a button to turn on the power from the battery, which must be activated before the measurement to avoid a high noise level from the power supply via USB. To the right there is a battery voltage indicator in millivolts, a field for recording the name of the recorded file and the size of the current recording.

When writing a file more than once, it is worthwhile to pay attention to the choice of another name, thereby avoiding the overwrite of the previous results.The colors of the channels on the charts: the first channel is red, the second is yellow (if the number of channels is not equal to two, the binding of color is different).

4.2 Device connection to subject

After the device is connected to the PC and checked for correctness of operation, it is necessary to connect it to the subject. To do this, first of all, you need to connect the correct wires to the leads of the multiplexer in the correct sequence. The terminals have the following sequence, from left to right: the first channel (current+, voltage+, voltage-, current-), the second channel (current+, voltage+, voltage-, current-), etc. (up to four). The sequence of connected wires must be taken into account for the correct subsequent placement on the test subject.

On the other end of the wires are connected to the electrodes. Since to improve the conductivity, the distance between the contacts should be minimal, the adhesive part of the electrodes must have a minimum width. The solution was to take ECG electrodes and cut to width. The limiting condition is the width of the snap of the wires. If the snap will protrude beyond the electrodes, with close placement of them to each other, the possibility of seizing and closing the leads is high. In this regard, the width of the electrode was chosen equal to the width of the snap - 15.5 mm.
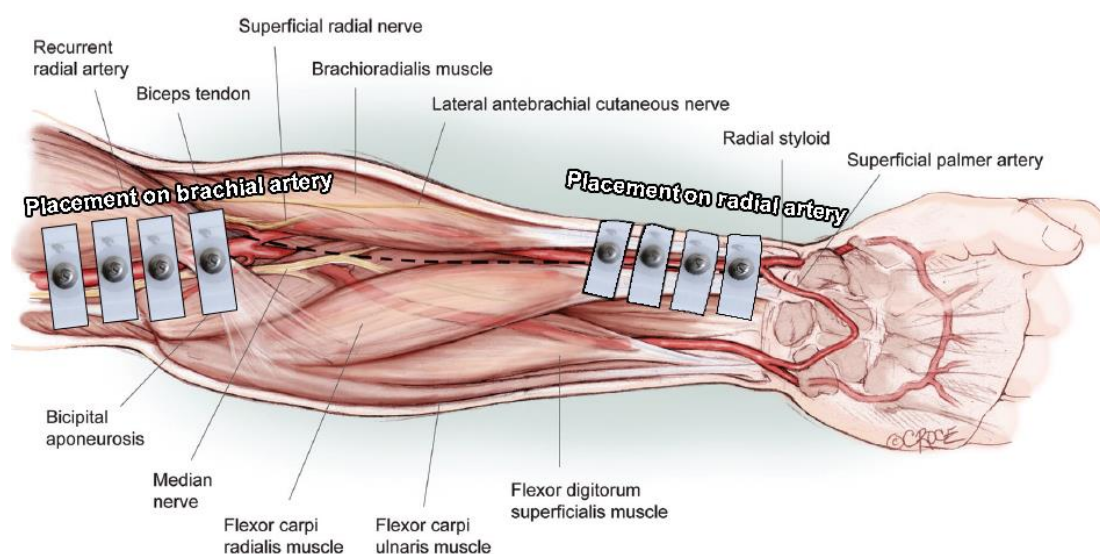
Figure 13. Scheme of electrodes' placement on the arm (both placement types on one arm – for PTT) [15]

The location of the electrodes is determined by the area of closest contact of the artery to the surface of the skin. The reference line for fixing the electrodes on the radial artery was a fold between the wrist and the forearm. The stickers are arranged in such a way that their central, conductive part is located at the place of proximity of the artery to the skin, i. e. along the outer boundary of the wrist. The stickers are placed parallel to the wrist fold at a distance of 3-5 mm from each other. In the case of PTT, one channel is connected over the brachial artery of the same hand. The reference line for the placement of electrodes is the elbow fold, on each side of which there are electrodes (paired on each side). They are placed at the same distance from each other along the inner border of the arm.

Apply the stickers to the skin by keeping them in a stretched state, so that the conductive area is tight against the skin.
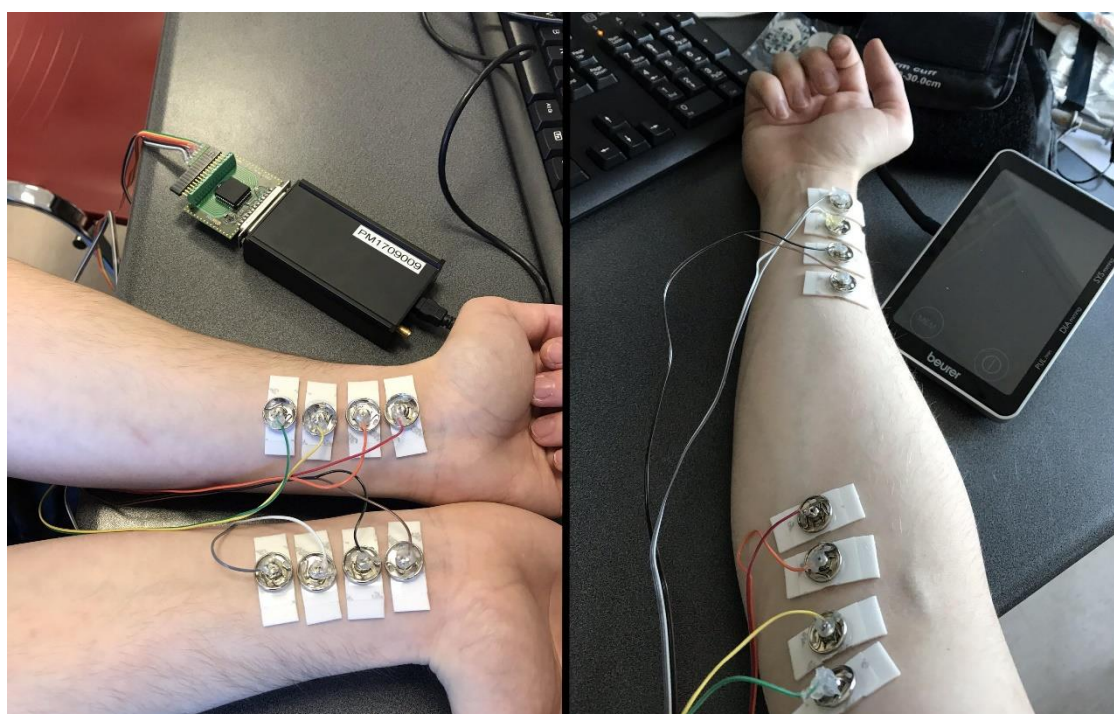
Figure 14. Photo of device connection to arms (left - for DPAT, right - for PTT)

Before the begin of the measurement procedure, the subject is measured by brachial pressure with the Beurer BM 58 and pressure is stored together with his data (gender, age).

4.3 Observation of oscillations

The main task at this stage is to get signals with a distinctly noticeable waveform visually similar to the theoretical one. Since the trends (offsets) on various channels are different - the Y-axis resolution on the amplitude-vs-time curve should be set to subtraction of the trend so that the amplitude of the oscillations could be distinguished.

The following criteria for sufficient signal quality were singled out:

- On each channel, the systolic and diastolic pulse fronts should be distinguishable.

- The gain and current gain scales do not reach the red area, what means that the current and voltage do not exceed the measurement limit. In the opposite case, it is worthwhile to check the electrodes in for a short circuit and to calibrate the amplification levels for a specific placement.

- The trend of the signal does not grow; otherwise check the quality of fixing the electrodes.

- Do not reduce the trend of the signal, otherwise check if the skin between the electrodes is dry and clean.

4.4 Result saving
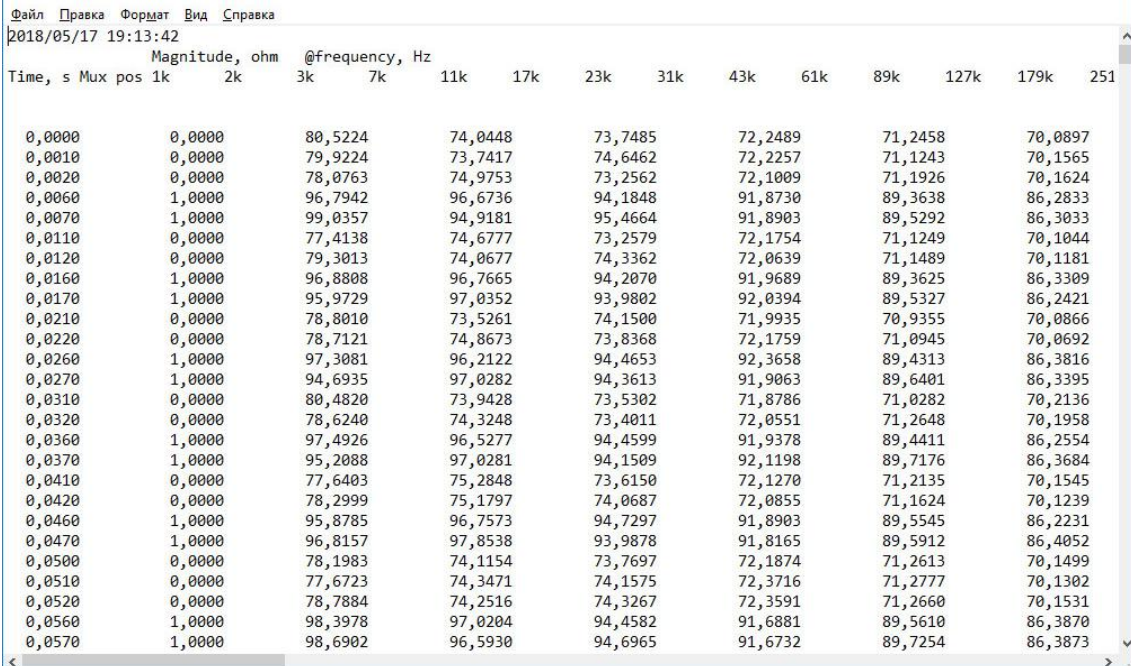
After completing the preparatory procedure and having ascertained the quality of the measured signal, the data must be recorded. Data is written to a text file in a folder in the root directory of the program for the measurements. First you need to make sure that in the "MUX Positions" parameter selected two channels. After making sure that under the current conditions the signal is obtained by the right shape, you should press the SAVE button at the bottom of the program interface to start recording and press again to finish recording. During the research, the recording time range was selected from 10 to 40 seconds, as the best for subsequent analysis. When recording time is less than 10 seconds, the signal, taking into account the 5 seconds transient response, becomes less than 5 seconds. This time is not enough for further analysis. When recording more than 40 seconds - Savitsky-Golay filter gets too high order and begins to perform incorrectly.

5 Collected data processing

To develop a measurements' file processing application, as the working environment was chosen - Mathworks MATLAB. The choice is conditioned by the fact that the MATLAB environment has ample opportunities for working with data matrixes, their processing and transformation, as well as for making plots. Another reason for choosing MATLAB is that I previously had experience with this program.

5.1 Data scan

Data is read from a text file. The file has a format in the form of a list of measurements, the time at which the measurement was made, its channel numbers, and the measured data itself (resistances and phases at 15 frequencies). Total - 32 columns, the number of lines depends on the measurement duration (approximately 200 lines per one second of measurements).


```
Файл  Правка  Формат  Вид  Справка
2018/05/17 19:13:42
           Magnitude, ohm   @frequency, Hz
Time, s Mux pos 1k      2k      3k      7k      11k      17k      23k      31k      43k      61k      89k      127k      179k      251

   0,0000          0,0000          80,5224          74,0448          73,7485          72,2489          71,2458          70,0897
   0,0010          0,0000          79,9224          73,7417          74,6462          72,2257          71,1243          70,1565
   0,0020          0,0000          78,0763          74,9753          73,2562          72,1009          71,1926          70,1624
   0,0060          1,0000          96,7942          96,6736          94,1848          91,8730          89,3638          86,2833
   0,0070          1,0000          99,0357          94,9181          95,4664          91,8903          89,5292          86,3033
   0,0110          0,0000          77,4138          74,6777          73,2579          72,1754          71,1249          70,1044
   0,0120          0,0000          79,3013          74,0677          74,3362          72,0639          71,1489          70,1181
   0,0160          1,0000          96,8808          96,7665          94,2070          91,9689          89,3625          86,3309
   0,0170          1,0000          95,9729          97,0352          93,9802          92,0394          89,5327          86,2421
   0,0210          0,0000          78,8010          73,5261          74,1500          71,9935          70,9355          70,0866
   0,0220          0,0000          78,7121          74,8673          73,8368          72,1759          71,0945          70,0692
   0,0260          1,0000          97,3081          96,2122          94,4653          92,3658          89,4313          86,3816
   0,0270          1,0000          94,6935          97,0282          94,3613          91,9063          89,6401          86,3395
   0,0310          0,0000          80,4820          73,9428          73,5302          71,8786          71,0282          70,2136
   0,0320          0,0000          78,6240          74,3248          73,4011          72,0551          71,2648          70,1958
   0,0360          1,0000          97,4926          96,5277          94,4599          91,9378          89,4411          86,2554
   0,0370          1,0000          95,2088          97,0281          94,1509          92,1198          89,7176          86,3684
   0,0410          0,0000          77,6403          75,2848          73,6150          72,1270          71,2135          70,1545
   0,0420          0,0000          78,2999          75,1797          74,0687          72,0855          71,1624          70,1239
   0,0460          1,0000          95,8785          96,7573          94,7297          91,8903          89,5545          86,2231
   0,0470          1,0000          96,8157          97,8538          93,9878          91,8165          89,5912          86,4052
   0,0500          0,0000          78,1983          74,1154          73,7697          72,1874          71,2613          70,1499
   0,0510          0,0000          77,6723          74,3471          74,1575          72,3716          71,2777          70,1302
   0,0520          0,0000          78,7884          74,2516          74,3267          72,3591          71,2660          70,1531
   0,0560          1,0000          98,3978          97,0204          94,4582          91,6881          89,5610          86,3870
   0,0570          1,0000          98,6902          96,5930          94,6965          91,6732          89,7254          86,3873
```

Figure 15. Raw data text file of measurements

The first 4 lines are preliminarily cut off, since they contain headers and names that are not necessary for further work. Information is recorded in 32 vertical arrays. The initially read data cells is written as a strings. Further, the resulting arrays are

29

rewritten in a two-dimensional matrix with a width of 32 columns and a height equal to the number of rows in one of the vertical arrays.

5.2 Data transformation

The string data type is converted into a numeric one, which allows further mathematical manipulation and plotting. One data packet contains two or sometimes three measurements; they need to be merged into one. Since the pairs of measurements go one by one for each channel in turn, this stage was combined with the separation of the rows to the corresponding by the channel matrixes. The source matrix is scanned by the channel column. If a change in the channel number is detected, the elements of the rows written to the buffer are summed up and divided by the number of rows (getting the average), then a new formed element is written into the new matrix corresponding to the channel number. This process continues until the end of the scanned matrix.

5.3 Filter design

The received signals had a high level of high-frequency noise; to obtain the primary signal - it needs to be cleared of noise. Considering that the frequency of the useful signal is not large relative to the frequency of noise, a Finite Impulse Response (FIR) filter with a Hamming window is suitable, as one of the common implementations of the digital filter. The specific feature of the window filter was the transient effect conditioned by that the filter window capturing values outside the signal's beginning (defined in MATLAB as zeroes). Considering that, before the further processing the segment at the beginning of the signal equal in length to one window of the filter was cut out after filtration.
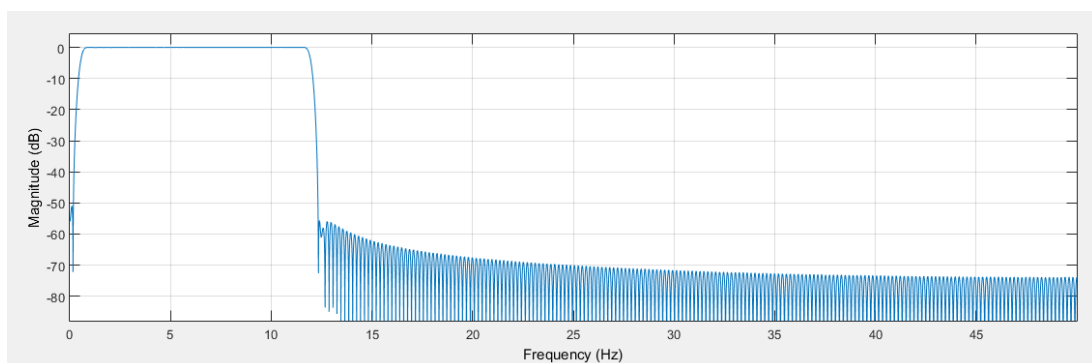
Figure 16. FIR-filter's passband plot

After analyzing the measured signals, I concluded that in the spectrum, apart from noise, four frequency components predominate. Among them: the trend, the heart rate, the rhythm of breathing and the second harmonic of the heart pulse. If the latter has a frequency higher than the pulse approximately twice and can be filtered together with noise, then the rhythm of breathing has a frequency below the pulse. Also should be removed the trend so that both signals are at the same level. Considering all this, it was decided to make a band-pass filter.

To calculate the upper cutoff frequency, an extremely high heart rate of 240 rpm was taken, which is 4 Hz. Since the pulse shape consists of two waves and has a rather steep first front, it was decided to take the cutoff frequency 3 times greater than the heart pulse frequency. It is assumed that three sample per period should be sufficient to maintain the recognizable waveform. Thus, the cutoff frequency of the calculated filter is 4×3=12 Hz. The lower cutoff frequency of the filter, in addition to the trend, must cover the breathing rate. The normal breathing rate is 15 breaths per minute and may vary in larger or smaller directions. However, since breathing can be controlled, in contrast to the heart rate, the cutoff frequency was taken as the minimum heart rate at 30 rpm or 0.5 Hz. Increasing the order of the filter by 2 times and monitoring the frequency response, it was determined that the maximum suppression is achieved at a value of 512 samples (further suppression changes insignificantly).
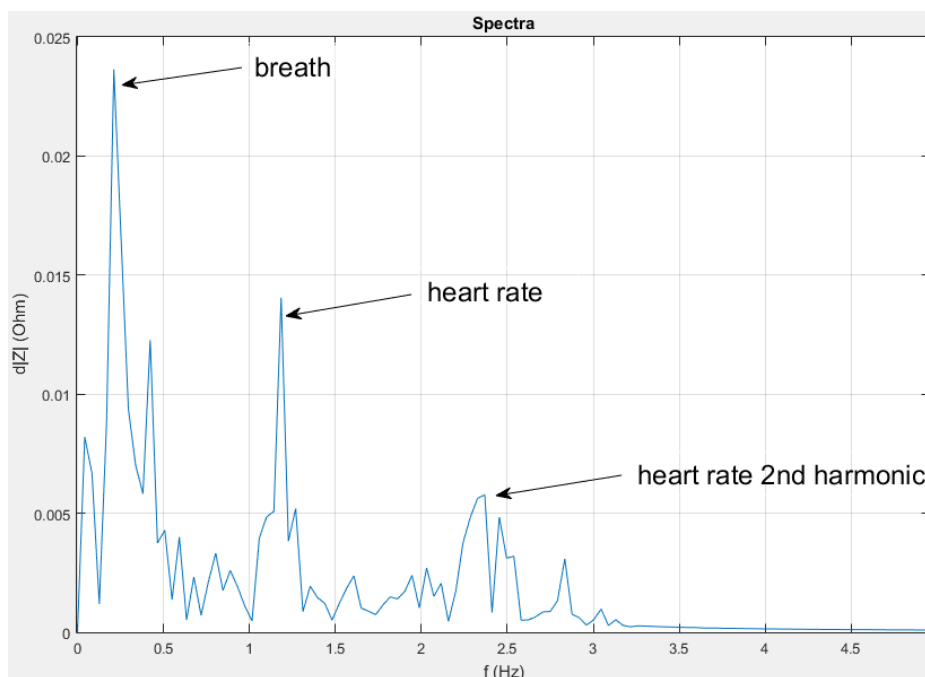
Figure 17. Frequency response after pre-filtration

The problem was the fact that the width of the lower band of suppression is very small (0.5 Hz). In combination with the fact that the amplitude of the breathing rate and the trend is much greater than the heart signal, it did not allow filtering out the low-frequency components for getting a qualitative cardiac signal. It was also not possible to take the cutoff frequency with a reserve, because the frequency of cardiac pulses in the spectrum is relatively close to the components that require removal. Considering all this, it was decided to apply additional high-pass filtering.

The window filter, as it turned out, does not give enough effect, and working with large filter orders would create a very large transient effect. It was decided to use a filter of a differentiating type, namely the Savitsky-Golay filter. The length of the window is selected the entire length of the signal, and the filter order takes the number of pulse waves in the signal and multiplies by 0.7 (the coefficient was chosen on an experimental basis), so that no absorption of the same pulse waves occurs. Further, the signal smoothed by the filter is subtracted from the initial signal to obtain high-pass filtering. Also, from the signal, the average value is subtracted to cut off the constant component before applying the Savitsky-Golay filter.
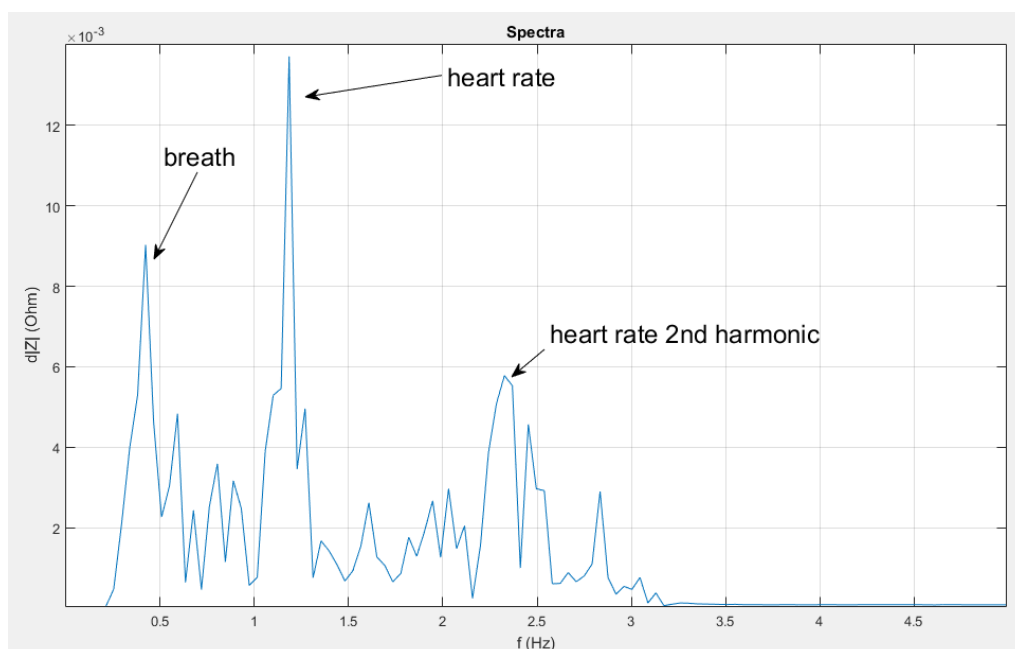
Figure 18. Frequency response after final filtration

5.4 Heart beat rate determination

A very informative indicator of CVS is the heart rate. In addition to the general idea of the heart activity, heart rate allows to set parameters for subsequent functions, such as the order of the filter or the width of the window.

To find the heart rate, the fast Fourier transform was used to extract the desired frequency component by the maximum value in the spectrum. Since the Savitsky-Golay filter order is calculated on the basis of data on the number of pulse waves, the pulse is calculated before its application, but after the FIR-filtering and subtraction of the mean. Considering this, the spectrum component corresponding to the breathing rate can exceed the pulse frequency in amplitude and be incorrectly determined as a heart rate. To avoid such an error, a threshold frequency of 30 rpm was taken, with a decrease in which the maximum is defined as the breathing rate. If this happens, that the value at the respiration rate exceeds the value at the heart rate, then the procedure for determining the second maximum would be started.
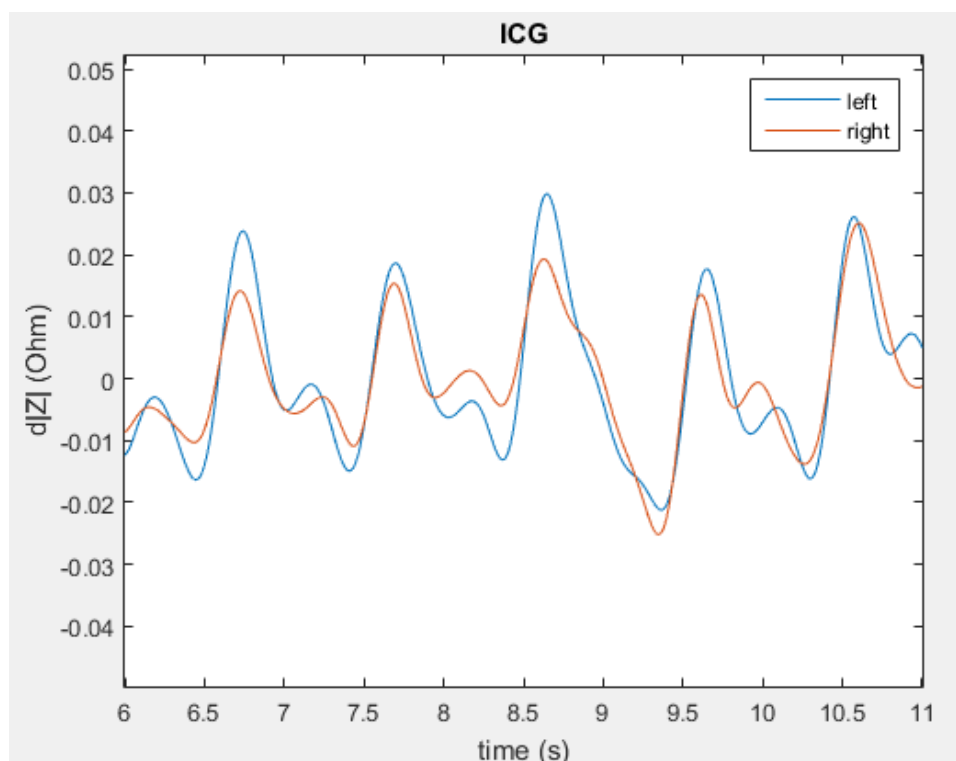
Figure 19. Amplitude-time plot of filtered signals from left and right hand

To find the second maximum, the entire spectrum is divided by frequency into segments with a length of 0.5 Hz. In each of the segments, the local maximum is determined. Among all the local maxima is the main one and the second highest. The second maximum becomes defined as the Heart rate. This division into segments is made to ensure that as the second maximum are not defined samples related to the first one (the samples describing the very highest peak).

5.5 Delays analysis

To calculate the delay between the signals, their cross-correlation was taken. If there is a delay between the curves, the maximum of the correlation function will also be shifted from the center by the same distance as the signals are separated from each other. This effect is conditioned by the fact that when one signal is shifted relative to the other by n samples, the maximum of the correlation function would achieved not in the middle, but in +n or -n. The signal has to be moved a distance of n more or less than for unshifted ones before they coincide. Whether n is positive or negative depends on whether the reference signal is lagging behind or comparable one. If $n < 0$, then the reference signal is ahead, if $n > 0$, then it lags behind.
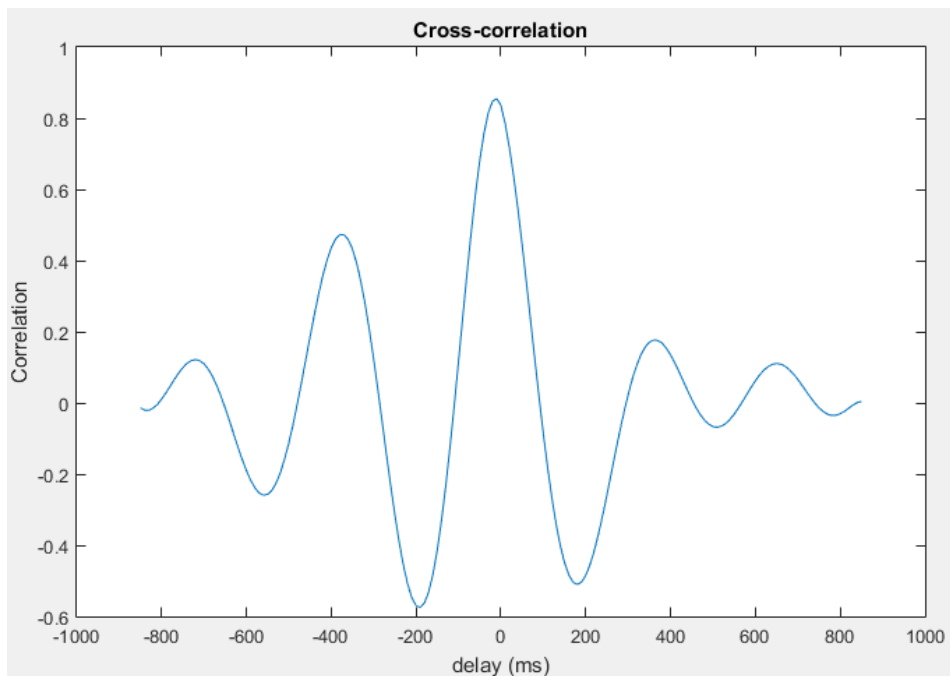
Figure 20. Cross-correlation function of signals from two hands

The error in calculating the delay is quite high due to the low resolution of the measuring device. The sampling is 10 ms, which is less than the range of the delay values by a factor of several. Taking into account that, according to the measurement results, the value of the delay varies in time, the cross-correlation of the whole signal can give too random a result. Thus, it was decided to compute cross-correlation on segments of a signal that is long in one period and in steps of one sample, including the values of delays into the array. By the array of delays for different segments, the median and the mean are taken further. For even greater completeness of the picture, it was decided to record an array of median and mean values obtained with the length of the cross-correlation window from one wavelength to the entire length of the signal. Taking now the average over the array of medians and over the array of means, we obtained numbers approximate to real delay.

6 Results of experiments

6.1 Format of results

During the investigation, 21 experiments were conducted for 4 subjects. The measurements were carried out using the PTT and DPAT methods, after which the pulse and delay were calculated. In addition to the impedance signal, the subjects measured the pressure with Beurer BM 58 pressure measuring device. As a result, the following data were recorded for each subject: gender, age, delay between signals by a median and by mean, upper and lower pressure, measured by a tonometer pulse and pulse, calculated on the basis of ICG measurements.

6.2 Result tables

Table 1. Subjects' data

Subject	Gender	Age
A	Male	22
B	Female	24
C	Male	39
D	Male	22

Table 2. PTT data for subject A

Subject	Experiment	Blood pressure	Measured Pulse	Calculated pulse	Delay by median	Delay by mean
A	1	118/75	109	113	-24	-7
A	2	116/77	104	102	-10	-3
A	3	132/75	111	103	-10	-3
A	4	143/83	134	132	-10	-48
A	5	161/97	156	135	-29	-23

Table 3. PTT data for subject B

Subject	Experiment	Blood pressure	Measured Pulse	Calculated pulse	Delay by median	Delay by mean
B	1	121/81	67	58	-4	-7
B	2	100/79	65	71	-35	-40
B	3	110//81	66	67	-33	-32
B	4	100/79	65	70	-50	-59

Table 4. PTT data for subject C

Subject	Experiment	Blood pressure	Measured Pulse	Calculated pulse	Delay by median	Delay by mean
C	1	124/82	82	88	-8	-8

Table 5. PTT data for subject D

Subject	Experiment	Blood pressure	Measured pulse	Calculated pulse	Delay	Delay
D	1	138/90	80	81	-16	-14

Table 6. DPAT data for subject A

Subject	Experiment	Blood pressure	Measured Pulse	Calculated pulse	Delay by median	Delay by mean
A	1	124/81	85	90	10	8
A	2	130/85	125	132	-37	-74
A	3	154/91	161	122	0	0

Table 7. DPAT data for subject B

Subject	Experiment	Blood pressure	Measured Pulse	Calculated pulse	Delay by median	Delay by mean
B	1	134/93	80	64	19	9
B	2	126/84	65	57	0	-4
B	3	118/80	71	69	-8	-8

Table 8. DPAT data for subject C

Subject	Experiment	Blood pressure	Measured Pulse	Calculated pulse	Delay by median	Delay by mean
C	1	124/82	82	89	0	0
C	2	141/94	103	101	23	68
C	3	179/93	135	126	28	77

Table 9. DPAT data for subject D

Subject	Experiment	Blood pressure	Measured Pulse	Calculated pulse	Delay by median	Delay by mean
D	1	153/84	91	86	-27	-26

6.3 Correlation charts

Figure 21.Correlation functions' plots of the dependence between brachial pressure and the time delay
of the pulse wave measured by the PTT method.
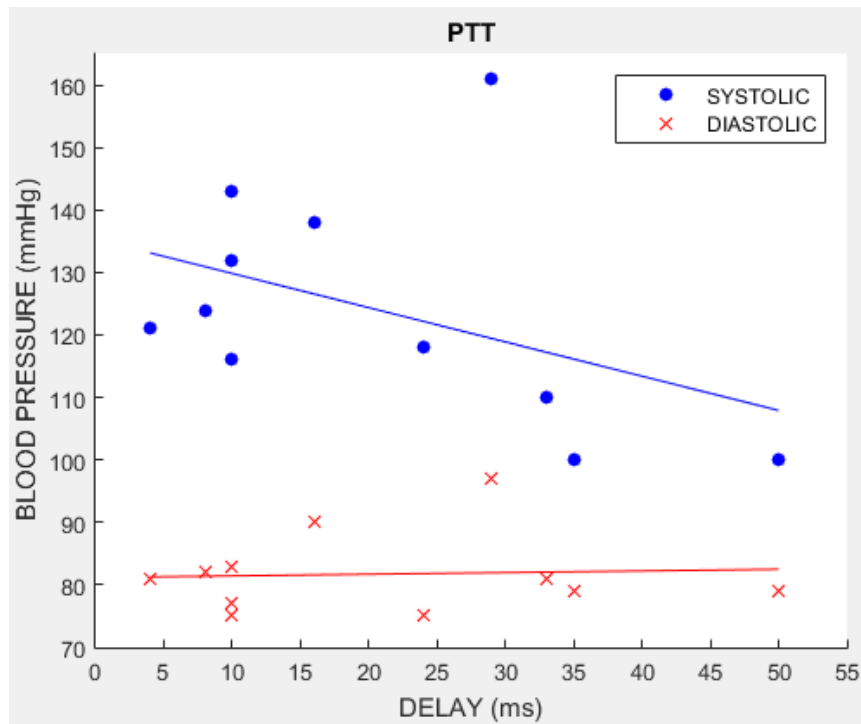**(Delay values were inverted to absolute values for clarity)**
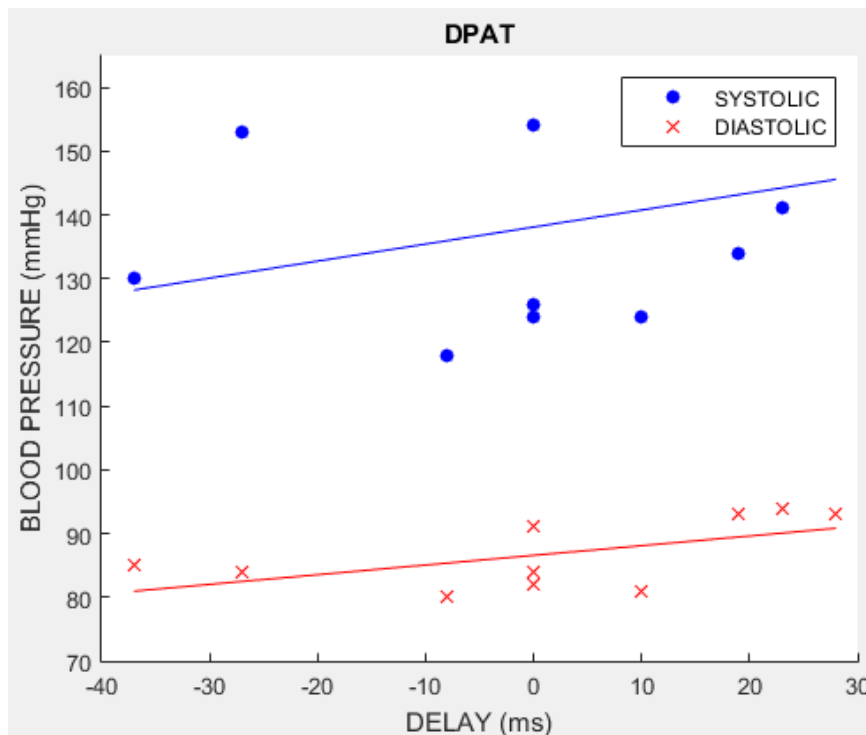
Figure 22. Correlation functions' plots of the dependence between brachial pressure and the time delay
of the pulse wave measured by the DPAT method

Table 10. Correlation coefficients

	PTT	DPAT
Systolic	-0.43	0.30
Diastolic	0.05	0.58

6.4 Results analysis

Based on the pressure and PTT delay values, it can be concluded that the delay varies mainly between 0 and 40 milliseconds. Normal pressure in the near the 120/80 corresponds to a low delay (0-10 ms), high, about 150/100 corresponds to a high delay (20-40 ms). Negative delay values for PTT indicate that the signal measured closer to the heart is ahead, and certain values for DPAT (since the reference signal was located on the left hand) correspond to expectations. Delays in measuring DPAT are similar in absolute values to PTT, but they are not always positive, which in turn indicates that the pulse wave does not always reach the right hand earlier than left hand. This may be due to the peculiarity of the structure of the body of various subjects, and within this thesis, it was not possible to find out the reasons. The speed of wave propagation can also be affected by the ratio of the volume of muscle cover on different arms.

The correlation was not absolute, but it is far from zero. For DPAT, with the increase in the systolic pressure, the delay time also increases, which indicates a positive correlation. This, while contradicting the elementary mechanics (with increasing speed the path time should decrease), gives an idea of the existing dependence. To understand this dependence, a more in-depth study of the biomechanical processes that arise and pass through the human CVS with a change in pressure is required. For PTT, an inverse dependence was found and does not cause any contradictions.

7 Summary

As a result of this investigation, a pulse wave was estimated with EBI method using the Quadra spectroscopic impedance analyzer. Was developed an application in MATLAB environment that allows the measured signal to be brought to the proper form and the heart rate to be determined. Furthermore, the program managed to fix the measurement delays by the PTT method (between two segments of one artery) and DPAT (between two parallel arteries) to find the correlation with the pressure. A correlation was obtained, though not completely in line with expectations (for DPAT), but indicating a certain dependence between pressure and delay. PTT, in its turn, gave expected and realistic dependence when with increasing of blood pressure time delay decreases.

To find a sufficiently accurate dependence - you should be used a device with a greater sampling rate of the measurable signal, then the one which Quadra possesses. With a sampling frequency of 100 Hz, Quadra has a measurement error of $\pm$ 10 ms, which is too much to fix the delays, counted in milliseconds, but it was enough to detect trends in their variations. By taking a device with a sampling frequency of at least 10 times (1 kHz) greater, it will be possible to measure the delay with an accuracy of 1 ms, which should be sufficient to detect the exact dependence between delay and pressure. Having studied in detail all biomechanical processes affecting the delay and modifying the procedure for its measurement, and also having acquired a device with a higher resolving power, it becomes possible to design a system that determines blood pressure based on impedance measurement.

Reference

[1] S. Connell, "Continuous Wearable Blood Pressure Monitor," 09 07 2016. [Online]. Available: https://contest.techbriefs.com/2016/entries/medical/6724. [Accessed 21 05 2018].

[2] M. Sharm, «Cuff-Less and Continuous Blood Pressure Monitoring: A Methodological Review,» 21 5 2017. [В Интернете]. Available: http://www.mdpi.com/2227-7080/5/2/21/htm. [Accessed : 21 5 2018].

[3] G. Cotter et al, "Impedance cardiography revisited," 05 07 2006. [Online]. Available: http://www.nicascardiocare.com.au/media/4849/Physiological-Measurement-2006-Impedance-cardiography-revisited.pdf. [Accessed 21 05 2018].

[4] Eliko, *QUADRA™ USER MANUAL,* Tallinn: Eliko, 2016.

[5] Renesas, "Renesas CD22M3494 DATASHEET," 05 29 2014. [Online]. Available: https://www.intersil.com/content/dam/intersil/documents/cd22/cd22m3494.pdf. [Accessed 21 05 2018].

[6] B. Schweber, "Med tech enhances wearables," 17 04 2017. [Online]. Available:https://www.embedded.com/print/4458291. [Accessed 21 05 2018].

[7] J. Hewes, "Impedance and Reactance," John Hewes , [Online]. Available: https://electronicsclub.info/impedance.htm. [Accessed 21 05 2018].

[8] smanuals.ru, "Цифровые измерители иммитанса E7-20/E7-25 и их применение," 30 04 2009. [Online]. Available: http://smanuals.ru/measurement-technology/immitance-measuring-instrument.html. [Accessed 21 05 2018].

[9] McEleavy OD *et al*, "Higher carotid-radial pulse wave velocity in healthy offspring of patients with Type 2 diabetes.," 21 03 2004. [Online]. Available: https://www.ncbi.nlm.nih.gov/pubmed/15008837. [Accessed 21 05 2018].

[10] Э.-Э. Мартинес, "Инструментальные методы исследования сердечно-сосудистой системы," [Online]. Available: http://www.serdechno.ru/instrumentalnye_metody_issledovaniya_serdechno-sosudistoy_sistemy/metody_issledovaniya_sosudistoy_sistemy/8222.html. [Accessed 21 05 2018].

[11] Д. Лужа, "Дуги Аорты," in *Рентгеновская анатомия сосудистой системы*, Книга по Требованию, 2012, p. 375.

[12] U. Birgersson, "ELECTRICAL IMPEDANCE," 2012. [Online]. Available: https://pdfs.semanticscholar.org/f3c5/539170aad1881377d9f5e5ed96fe38e07566.pdf. [Accessed 21 05 2018].

[13] Р. Всеволод, "СИНАПСЫ И НЕЙРОМЕДИАТОРЫ," Рудашевский Всеволод, [Online]. Available: http://bodhi.name/ru/zhivomordnost/%E2%98%B5sinapsy-i-nejromediatory/. [Accessed 21 05 2018].

[14] "Mean Arterial Pressure Calculator," 19 03 2011. [Online]. Available: http://www.physiologyweb.com/calculators/mean_arterial_pressure_calculator.html. [Accessed 21 05 2018].

[15] Arie Blitz *et al*, "Harvesting the radial artery," 07 2013. [Online]. Available: http://www.annalscts.com/article/view/2418/3284. [Accessed 21 05 2018].

Appendix 1 – MATLAB code

```matlab
%%source data format
filename = 'raw_data_log.txt';
delimiter = '\t';
startRow = 4;
formatSpec =
'%s%s%s%s%s%s%s%s%s%s%s%s%s%s%s%s%s%s%s%s%s%s%s%s%s%s%s%s%s%s%s%s%[^\
n\r]';

%% data scan
fileID = fopen(filename,'r');

titles = textscan(fileID, '%[^\n\r]', startRow-1, 'ReturnOnError',
false);
dataArray = textscan(fileID, formatSpec, 'Delimiter', delimiter,
'ReturnOnError', false);

fclose(fileID);
%% making empty matrix
matrix = repmat({'0'},length(dataArray{1}),length(dataArray)-1);


%% fill the matrix
  for col=1:length(dataArray)-1
      matrix(1:length(dataArray{col}),col) = dataArray{col};
  end

%% converting matrix's elements from char string to float

for col=[1:32] % external loop

    colArray = dataArray{col};

    for row=[1:size(colArray)]; % internal loop

            element = matrix(row,col);

                element = strrep(element, ',', '.'); % change
separator
                element = str2double(element);  % to numeric

              matrix{row, col} = element;
    end
end

%% channel division and packet merging

channel_ID = str2double(strrep(dataArray{2}, ',', '.'));
```

```matlab
mx_col = 1;

for col=[1,3:32] % external loop



  m0_row = 1;
  m1_row = 1;
  m2_row = 1;
  m3_row = 1;
  row = 1;

        while (row < size(colArray,1)) % internal loop


            buff_row=1; % buffer's element

                buffer(buff_row) = matrix(row,col); % first element

                while (row < size(colArray,1) && channel_ID(row) ==
channel_ID(row+1)) % if packet's channel is equal to next packet's
channel and is not the last


                    buffer(buff_row+1) = matrix(row+1,col); % add the
next element
                    buff_row=buff_row+1;
                    row=row+1;
                end

                packet_avg=mean(cell2mat(buffer));
                clear buffer

                  if (channel_ID(row)== 0)
                            matrix_0{m0_row, mx_col} = packet_avg;
                            m0_row=m0_row+1;

                        elseif (channel_ID(row)== 1)
                            matrix_1{m1_row, mx_col} = packet_avg;
                            m1_row=m1_row+1;

                        elseif (channel_ID(row)== 2)
                            matrix_2{m2_row, mx_col} = packet_avg;
                            m2_row=m2_row+1;

                        elseif (channel_ID(row)== 3)
                            matrix_3{m3_row, mx_col} = packet_avg;
                            m3_row=m3_row+1;
                  end
            row=row+1; % raise the row
        end
        mx_col=mx_col+1; % raise the new matrixes's column
end

%% FIR-filter adjust
fc1 = 0.5/100/2; %cutoff_freq1
fc2 = 12/100/2; %cutoff_freq2
order = 512
win = hamming(order+1);
h = fir1(order, [fc1 fc2], win);
```

```matlab
%% Pre-filtering


A = order % plot starts at
B = length(matrix_0(:,1)) % plot ends at

% selected frequency - 23 kHz
y = cell2mat(matrix_0(:,7));

z = cell2mat(matrix_1(:,7));

t = cell2mat(matrix_0(A:B,1)); % timeline

  y = filter(h,1,y);
  z = filter(h,1,z);

y = -y(A:B); % inversing the signal
z = -z(A:B); % inversing the signal
y = y-mean(y); % delete dc component
z = z-mean(z); % delete dc component

 %% Heart Beat Rate



L = length(t)          % Length of signal
Fs = 100;              % Sampling frequency
T = 1/Fs;               % Sampling period



spectr=fft(z) % to spectral form
spectr2S= abs(spectr/L);  % normalize the curve
spectr1S= spectr2S(1:L/2+1); % from 2-side band to 1-side band

spectr1S(2:end-1) = 2*spectr1S(2:end-1);

f = Fs*(0:(L/2))/L;


            figure(2)
            plot(f,spectr1S)
            title('Spectra');
            xlabel('f (Hz)')
            ylabel('d|Z| (Ohm)')


[HBR_value, HBR_pos]= max(spectr1S)
HBR = round(f(HBR_pos)*60, 0)
% checking if breathing impact has grater amplitude than heart beat
if   HBR < 30
    Breath_rate = HBR

    % 30 BPM length window
    f1 = 1                          % window begin
    Wsz = roundn(0.5/f(2),+0)+1 % window size
    f2 = Wsz                        % window end
    i = 0                           % cicle iteration number
```

44

```matlab
    while f2 <= length(spectr1S)     % finding local maximums of
spectra

        [HBR_value, HBR_pos] = max(spectr1S(f1:f2)); % choice local
maximum on interval

        lmax(i+1) = HBR_value;
        lmax_pos(i+1) = HBR_pos+Wsz*i;

        f1=f1+Wsz;
        f2=f2+Wsz;
        i=i+1;
    end

    [max2, max2_pos]= max(lmax(lmax<max(lmax))); % taking 2nd maximum
meaning

    max2_pos= lmax_pos(max2_pos+1)
    HBR = round(f(max2_pos)*60, 0) ;

end

waves= length(t)*0.01*HBR/60 %wave quantity
%% Post-filtering


 y = y-mean(y) % delete dc component
 signalsize=length(y);

 if mod(signalsize,2) == 0 ;
    signalsize = signalsize-1 ;
 end
 sg_order = 0.7*waves ; % 0.7 of wave quantity
 sg_order = roundn(sg_order,-0) ;
 y_dc = sgolayfilt(y,sg_order,signalsize); % precise adjust dc
component
  y = y-y_dc;


 z = z-mean(z) % delete dc component

 z_dc = sgolayfilt(z,sg_order,signalsize); %precise adjust dc
component
  z = z-z_dc;

            figure(3)
            plot(t, y, t, z)
            title('ICG')
            legend ('left', 'right')
            xlabel('time (s)')
            ylabel('d|Z| (Ohm)')


 %% Delays

 for j = 1:waves
    if B - order - j*round(L/waves,0) > 0
```

```matlab
        cwindow = j*round(L/waves,0); % corralation chart window
width

        ss_end = B - cwindow - order;
        clear delay;

            for ss = [1:ss_end] % ss = start sample

                    yw = y(ss:ss+cwindow);   % N
                    yw = yw / norm(yw);      % O
                    zw = z(ss:ss+cwindow);   % R
                    zw = zw / norm(zw);      % M

                [cor, lags] = xcorr(zw,yw);

                [maxcor, lag] = max(cor);
                delay(ss) = 10*lags(lag);
            end

        med_arr(j) = median(delay);
        avg_arr(j) = mean(delay);

    end
 end


 med = round(mean(med_arr),0)
 avg = round(mean(avg_arr),0)

        figure(4)
        plot(t(1:ss_end),delay);
        title('Delays curve');
        xlabel('time (s)')
        ylabel('delay (ms)')

clearvars -except med avg HBR
```